Modeling and Analysis of Undersea Capacitive Power Transfer Based on Conduction Current in Seawater

Xichen Liu, *Student Member, IEEE*, Chunwei Cai, *Member, IEEE*, Shuai Wu, *Member, IEEE*, Chenghao Li, *Graduate Student Member, IEEE*, Qinyuan Cui, and Xiuyun Ren, *Member, IEEE*

***Abstract*—The liquid environment and high conductivity of the seawater, which changes the characteristic of capacitive coupler compared to the air condition, are the difficulties to adoption of capacitive power transfer (CPT) technology for marine device. In this article, a universal circuit model of the bipolar plate fully immersed into water environment is proposed and divided into three cases based on the conductivity, validating the conduction path dominates the capacitive coupling in seawater. Then, the theoretical model of undersea four-plates coupler immersed into seawater, which consists of four coupling capacitances between metal plate and seawater and six seawater resistances, is derived, analyzed, and simulated. It well explains the reason of stable parameters of the coupler and power mainly flowing in receiving side since coupling object is seawater rather than plate. Later, a seawater CPT system with Y-type capacitor and single wire is proposed for realizing efficient power transmission. Finally, a laboratory prototype is established and achieves stable 171 W and 85% dc–dc efficiency with lower than 1% variation under random misalignment.**

***Index Terms*—Capacitive power transfer (CPT), conduction current, seawater, single wire.**

I. Introduction

CURRENTLY, wireless power transfer (WPT) technology, with characteristics of convenience and noncontact, is widely applied in the field of power supply [1]. As for marine environment, the potential risks of short circuit and insertion wear caused by the liquid corrosion condition require a safe and effective charging solution for autonomous underwater vehicles or sensor networks [2].

Received 10 August 2024; revised 18 October 2024; accepted 11 November 2024. Date of publication 13 November 2024; date of current version 26 December 2024. This work was supported in part by the Major Scientific and Technological Innovation Project of Shandong Province of China under Grant 2022ZLGX04, in part by the National Natural Science Foundation of China under Grant 52401406, and in part by the Taishan Scholars of Shandong Province under Grant tsqnz20240801. Recommended for publication by Associate Editor M. Ponce-Silva. *(Corresponding author: Xiuyun Ren.)*

Xichen Liu, Chunwei Cai, Shuai Wu, Chenghao Li, and Xiuyun Ren are with the College of New Energy, Harbin Institute of Technology-Weihai, Weihai 264209, China, and also with the Key Laboratory of Cross-Domain Synergy and Comprehensive Support for Unmanned Marine Systems, Ministry of Industry and Information Technology, Weihai 264209, China (e-mail: 21s030155@stu.hit.edu.cn; caichunwei@hit.edu.cn; wushuai@hit.edu.cn; 23b906007@stu.hit.edu.cn; renxiuyun_78@163.com).

Qinyuan Cui is with the Hangzhou Power Supply Company of State Grid Zhejiang Electric Power Company, Ltd., Hangzhou 310000, China (e-mail: cuiquance@163.com).

Color versions of one or more figures in this article are available at https://doi.org/10.1109/TPEL.2024.3498063.

Digital Object Identifier 10.1109/TPEL.2024.3498063

Inductive power transfer (IPT) and capacitive power transfer (CPT), utilizing magnetic or electric field as medium, are the mainstream technologies for wireless high-power transmission. According to [3], the eddy loss of the seawater in IPT system under low frequency can be nearly ignored, leading to better transfer performance in [4]. However, the metallic shell of the charging object used to resist high pressure in deep sea will inevitably produce high eddy loss in IPT system, hindering its further applications. Therefore, the CPT technology seems more suitable since it can achieve power transfer across metals through electric field and seawater possesses high relative permittivity [5], [6]. But, different from air condition, both of liquid environment and high conductivity will change CPT system characteristic, especially for the aspects of coupling mode and current path in the water. It makes the CPT system difficult to be used for applications.

According to the ion concentration and composition, liquid environment can be divided into pure water, freshwater, saline, tissue fluid, seawater, etc. They possess different conductivity and corrosivity, showing different performance. Therefore, to explore the characteristics of the CPT system in the liquid environment, scholars have made many efforts. Urano et al. [7] take one electrode isolated from water and another electrode exposed in freshwater to construct a power loop with L-L resonant network, resulting 19.8 mW with efficiency of 76.7% in 700 kHz. It points that the uninsulated electrode, composed by two metallic plates in water, will form the electric double layer (EDL) in the surface and then work as an RC circuit which the performance of it will be influenced by the ion concentration in water. Likewise, two exposed electrodes are set in freshwater and a kQ-product theory about frequency is proposed for efficiency improving in [8] and [9]. And then, the system efficiency of electromagnetic simulation and theoretical calculation at 94 MHz with changing conductivity of water are compared. It shows that the water with the conductivity in more than 0.2 S/m cannot be completely treated as dielectric. However, the safety of uninsulated coupler is hard to guarantee due to the persistent corrosion and potential electric breakdown. So, Zhang and Lu [10], [11] consider the impact of the insulation of coupler and give a circuit model of the insulated two-plate in freshwater, which is composed by two coupling capacitances across insulation and one coupling capacitance across water. Basing on the high relative dielectric of water, a long-distance underwater CPT system is achieved with 219.6 W power over 500 mm distance. But the system efficiency is only 60.17% which the loss of coupler is 88 W accounting for

60.49%. Also, a *LC-CLL* compensation topology is applied in fresh water CPT with an efficiency of 36% in constant current and an efficiency of 44% in constant voltage mode separately [12], indicating the freshwater is a lossy dielectric compared to air. To address this defect to improve system performance, Rong et al. [13] propose a hybrid-dielectric coupler composed by air as the filling dielectric and fresh water as the transfer dielectric to optimize the coupling coefficient. In other words, low relative dielectric constant material is used to reduce self-capacitance and high relative dielectric constant material to enhance mutual capacitance. Finally, a 5-kW prototype with 87.2% efficiency is established accompanied with relative insensitivity to misalignment.

These research work have demonstrated the coupling mode of the fresh water with the conductivity of 0.0002 S/m is like the air except for the high relative dielectric, necessary insulation, and inevitable loss. Accordingly, the air study about coupler structure and compensated topology can still be utilized. However, as the conductivity of the liquid increases, the coupling mode of capacitive coupler changes and proportion of conduction path in water increases [14]. Besides, many important underwater equipment is in the ocean full of seawater with the conductivity of 3–6 S/m. Hence, the research of seawater needs to be reconsidered.

The exposed electrode is first used in seawater CPT (SCPT) system in [15], [16], and [17] with an efficiency of 85% in 11.87 kHz. It is reported that the seawater can behave as a conductor over 700 Hz. At this case, while the surface of the metallic plate will form an EDL leading to a high Q-factor, electrolytic reaction has limited the plates voltage to a minimum value, that is, the power capacity can be only milliwatts. Meanwhile, the corrosion environment also lets accurately characterizing the underwater power channel hard. Hence, a capacitive coupler with two pairs of parallel-plate electrodes with insulation coatings-polyimide tape are built in [18]. It clarified the operational principle of the conductive coupler using theory derivation based on simplified equivalent circuit and establish a WPT system, achieving the efficiency of 50% at 6.78 MHz with an input power of 275 W and 5 mm transfer distance. For further research, Tamura et al. [19] put the coupler into seawater environment attaching to the support substrate with insulation coating and give an equivalent circuit model of the coupler. It points that the conductive coupling is dominant in seawater, resulting in that the self-coupling is so strong that the current flows almost entirely on the emission side. Hence, to shield this impact, a partition damper dividing seawater into two parts is designed to achieve 1 kW system with the efficiency of 93% at 20 mm and 85.3% at 150 mm. Furthermore, the actual environment is considered and both of cases could be maintained 94% up to10 MHz, indicating the conductive coupler is suitable for the case when unmanned underwater vehicles landed on the charging station. However, when a conductive material is employed as the outer shell of charging object, there will be a large amount of high-frequency current leaking out, leading to the decrease of efficiency. Also, two seawater bags are utilized as medium placing between the transmitting and receiving plates in [20] and the paper [21] takes dual-cavity to separate the transmitting and receiving electrode. The purpose of these mechanical isolation methods is to cut off self-coupling path in four-plate system, pointing the current flowing in the seawater is conduction current not displacement current. Considering a high seawater pressure in the actual seawater environment and conductive shell of the charging object, the physical isolation design is challenging and difficult to prevent the high-frequency current leakage. So, the operational principle of seawater coupler for the marine equipment with conductive shell, namely fully immersed into a united seawater environment needs further research.

Due to a short history, the basic theory research of SCPT technology is insufficient and the existing research is limited to constrained self-coupling by mechanical method. So, this article first proposes a universal circuit model of the bipolar plate immersed into water environment considering varied conductivity of water to comprehensively elucidate the coupling mode and the distribution law of the displacement and conduction current path of the SCPT system in Section II. And then, a special coupling mode of undersea capacitive coupler with four independent coupling capacitance and conduction current path in seawater with six-resistances are revealed to explain the power path in Section III. Finally, in Section IV, a SCPT system with Y-type capacitor and single wire is proposed and constructing a laboratory prototype in hardware. In addition, an actual ocean experiment is also tested, validating the analysis. The contributions of this article can be clarified as follows.

1) Giving three cases of the coupling mode of the capacitive coupler immersed into water with different conductivity. By theory model, validating that the conduction path dominates the capacitive coupling in seawater.
2) Updating the equivalent circuit of seawater coupler under full immersion, describing the power transfer ability of SCPT system. Revealing traditional four-plates SCPT system hard to realize high-power transfer since power mainly flowing in primary side and random transmitting.
3) Proposing a conductive SCPT system with Y-type capacitor and single wire. Constructing laboratory and actual ocean experiments separately to validate the analysis in this article.

II. Law of Displacement and Conduction Current Distribution of Underwater Capacitive Coupler With Varied Conductivity

A. Universal Composition of Underwater Bipolar Plate Current Path

Considering the different kinds of water such as pure water, freshwater, and seawater show different electrical conductivity, possessing unique characteristics, the current flowing through water in the capacitive coupler is various. For clarifying the current path in water, this article applies two metallic plates P_1 and P_2 with insulation into the water based on software COMSOL, shown in Fig. 1(a). The insulation is on the surface of the plates and capacitive coupler dimensions are listed in Table I. To reduce analysis complexity, the square plates are chosen and their thickness is set small since it has a certain impact on the coupling based on the edge effect.

Taken both the direct coupling model of capacitive coupler in multimedium and water resistance into account, this article proposes a universal circuit model of the bipolar plate in water

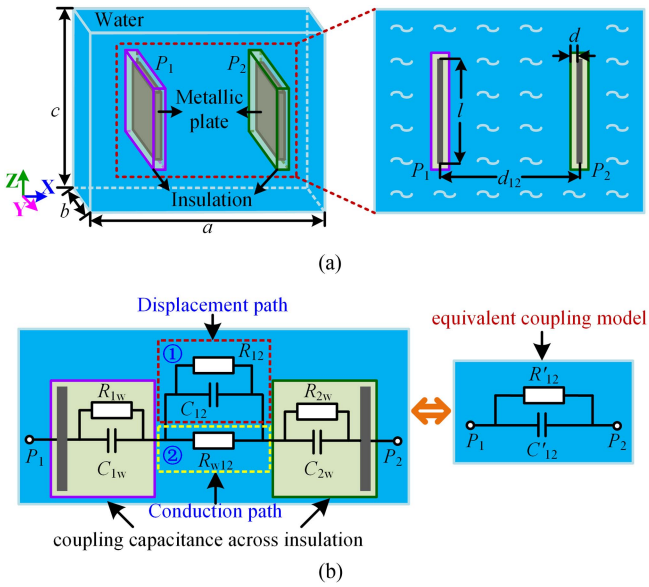

Fig. 1. (a) General overview of the bipolar plate. (b) Universal circuit model of the bipolar plate in water environment.

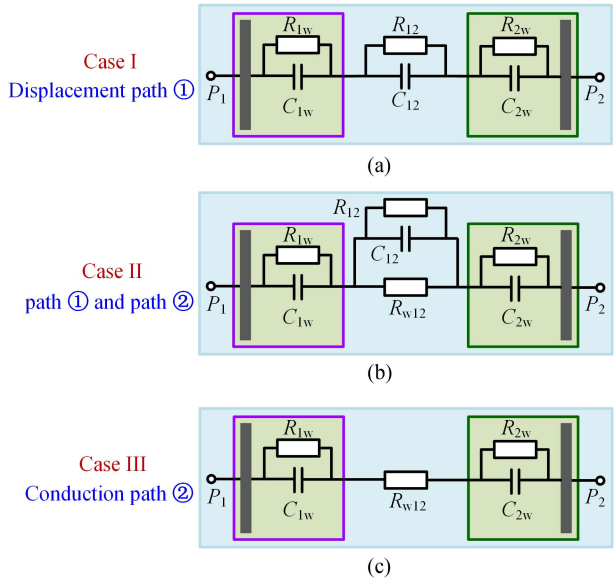

Fig. 2. Current path distribution. (a) Water as medium. (b) Water as medium and conductor. (c) Water as conductor.

TABLE I
DIMENSIONS IN A BIPOLAR PLATES CAPACITIVE COUPLER IN WATER

Parameter	Defined	Parameter	Defined
a	Water length	d_{12}	Plate distance
b	Water width	d	Insulation thickness
c	Water height	l	Plate length

environment, as shown in Fig. 1(b). There are displacement path ① and conduction path ② working together in water, exhibiting as the capacitance C_{12} and water resistance $R_{\mathrm{w}12}$. Namely, the water acts as both medium and conductor. The coupling capacitances across insulation are defined as $C_{1\mathrm{w}}$ and $C_{2\mathrm{w}}$. Besides, the parasitic resistance of the capacitors is also taken into consideration in the model for accurately describing the power loss, resulting in resistances as $R_{1\mathrm{w}}$, $R_{2\mathrm{w}}$, and R_{12}.

Although the equivalent capacitance C'_{12} and resistance R'_{12} can be derived as (1) to reduce complexity of analysis, it is needed to be pointed that the components are not constant and only used to describe universal characteristics. Their value and existence will be changed under the different conductivity of water and excitation frequency since varied ion response condition and ion concentration lead to the water shifting in medium property and conductor property

$$\begin{cases} C'_{12} = \frac{C_{1\mathrm{w}}C_{2\mathrm{w}}C_{12}}{C_{1\mathrm{w}}C_{2\mathrm{w}}+C_{1\mathrm{w}}C_{12}+C_{2\mathrm{w}}C_{12}} \\ R'_{12} = R_{1\mathrm{w}} + R_{2\mathrm{w}} + \frac{R_{\mathrm{w}12}R_{12}}{R_{\mathrm{w}12}+R_{12}} \end{cases}. \tag{1}$$

In further analysis, there are three cases according to water property, as shown in Fig. 2.

Case I: In case I, medium property of water dominates the capacitive coupling. Therefore, there are only two conductors plate P_1 and P_2 leading to one coupling capacitance, which contains three parts divided by the medium of insulation and water, existing through displacement path ① in water. At this time, the effect of the conduction path ② is small to be ignored.

Case II: In case II, both medium property and conductor property of water dominate the capacitive coupling. That is the displacement path ① and conduction path ② cannot be ignored. And their contribution proportion will change with electrical conductivity of water and excitation frequency. At this time, it is hard to distinguish the coupling state.

Case III: In case III, conductor property of water dominates the capacitive coupling. It can be seen that since the conductor water fully wraps the conductor plate P_1 and P_2, there are two main coupling capacitances across insulation connected by the conduction path ②. At this time, the effect of the displacement path ① is small to be ignored.

Based on the analysis, it can be pointed that the excitation frequency, conductivity and relative dielectric constant of water, insulation material and thickness and metallic plate area are important parameters determining the coupler characters.

B. Analysis of the Underwater Bipolar Plate

To illustrate the analysis, a finite element simulation model is constructed. The size of bipolar plate is initially selected to be 300 × 300 × 10 mm and the distance between them is 100 mm. The soda lime glass with the relative dielectric constant of 7.4 is used to cover plates as insulation layer in 1 mm. In this design, the region of water is set 3000 × 3000 × 3000 mm and its conductivity σ and relative permittivity $\varepsilon_{\mathrm{r\text{-}water}}$ are changed in a large range respectively to observe the variation of equivalent coupling parameter under 300 kHz and 6.78 MHz excitation, as shown in Fig. 3.

It can be pointed out that compared with 300 kHz, the high excitation frequency such as 6.78 MHz delays the effect of conductivity on the capacitive coupling state. Further reasons

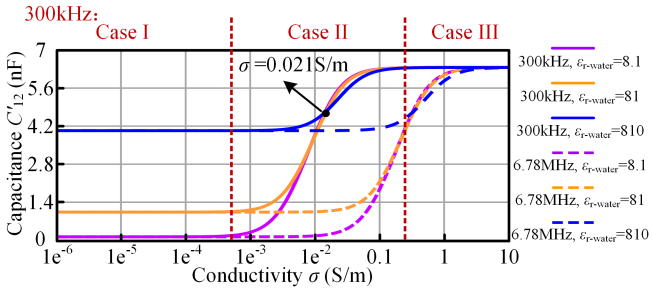

Fig. 3. Equivalent capacitance variation under different conductivity and relative permittivity of water and excitation frequency.

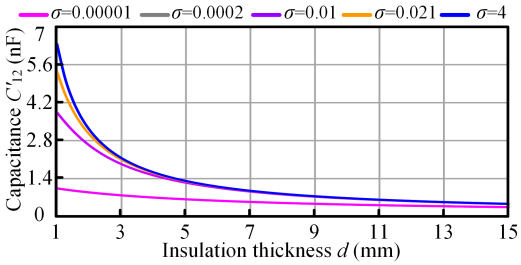

Fig. 4. Equivalent capacitance variation under different insulation thickness.

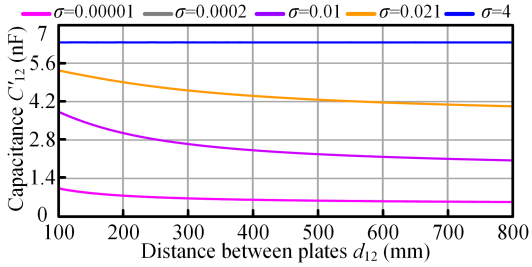

Fig. 5. Equivalent capacitance variation under different transfer distance.

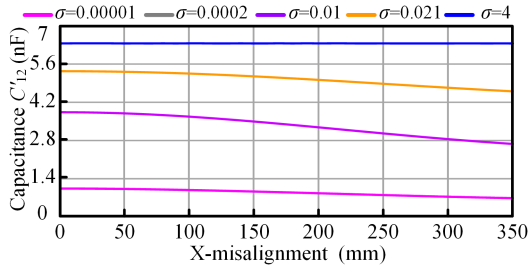

Fig. 6. Equivalent capacitance variation under x-misalignment.

are complicated in microscopic view, such as the structure and motion of ions [22]. Meanwhile, the impact of the parasitic parameter at high excitation frequency is also great. Therefore, to reduce additional interference, this article chooses 300 kHz as example for describing. At this time, in Fig. 3, the region can be divided into three parts according to previous analysis. In case I, the conductivity is lower than 0.0001 S/m. It is obvious that equivalent capacitance C'_{12} is only affected by relative permittivity, which verifies the displacement path ① dominant in water. As for case II, the range of conductivity is from 0.0001 to 0.5 S/m, where C'_{12} is determined not only by the conductivity but also by the relative permittivity. It validates that the path ① and path ② work together and the contribution of path ① is gradually decrease to 0. When the conductivity higher than 0.5, the region is regarded as case III and C'_{12} is independent from σ and $\varepsilon_{\text{r-wate1r}}$, showing the water is regarded as a conductor. The stimulation results have partially validated the analysis in Fig. 2. To further observe the performance of underwater bipolar plate, the equivalent capacitance performance about insulation thickness, distance between plates, plate length, and misalignment are all tested under the chosen representative conductivity of 0.00001, 0.0002 (freshwater), 0.01, 0.021, and 4 (seawater).

When the insulation thickness d varies, the stimulation result is shown in Fig. 4. The curves of $\sigma = 0.00001$ and $\sigma = 0.0002$ are nearly coincided, indicating the freshwater can be regarded as medium unless electrolytic reaction occurs, which is consistent to the previous research. While the capacitance will decrease under all conditions as d increases, the reasons for dropping are totally different considering the roles of water switching. For instance, when the insulation thickness is 1 or 4 mm, the capacitances are separately 6.36 and 1.63 nF, similarly to four times, under the conductivity of 4 S/m. It is consistent to the feature of coupling capacitances formed between plate and seawater in case III. As for the others conductivity, it can be mainly attributed to the hybrid-dielectric coupler according to [13] in case I and hybrid property of water in case II.

The impact of the distance between plates d_{12} is also tested and shown in Fig. 5. The insulation thickness is 1 mm in this analysis. Except for the conductivity $\sigma = 4$, the capacitances are all significantly affected by the distance in different condition, exhibiting the characteristic of water medium. It demonstrates that two coupling capacitances in seawater are formed between plates and corresponding seawater on the surface of insulation and then connected by seawater, nearly independent to transfer distance. But, due to the lack of high conductivity compared to metal, the seawater resistance will be taken in consideration.

The misalignment performance is also simulated and the results are depicted in Fig. 6. The distance between plates is 100 mm. Likewise, when the Y-direction misalignment occurs, in addition to the seawater, the equivalent capacitance C'_{12} is influenced. Of course, in any case the change is less than air. For example, at $\sigma = 0.01$ and 200 mm misalignment, C'_{12} varies from 3.84 to 3.3 nF, showing strong misalignment tolerance.

Basing on the above-mentioned analysis of the model, the seawater can be regarded as a conductor in coupling mode under 300 kHz. At this case, the equivalent capacitance C'_{12} is composed by the coupling capacitance $C_{1\text{w}}$ and $C_{2\text{w}}$ generated between metal plate and seawater across insulation layer. Their value and corresponding parasitic resistance $R_{1\text{w}}$ and $R_{2\text{w}}$ can be obtained by (2), showing not affected by the transfer distance and misalignment. It is noted that considering the influence of the surrounding seawater, the area of metal plate consists six faces. In future study, the water with $\sigma = 0.001$–0.1 will be further discussed and contribution proportion of displacement path ①

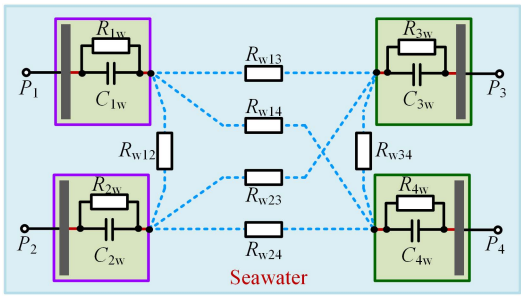

Fig. 7. Circuit model of undersea four-plates coupler.

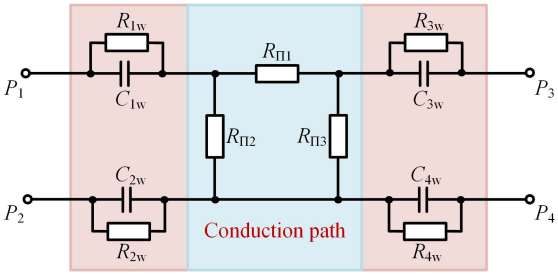

Fig. 8. Equivalent Π-resistances model.

and conduction path ② will also be paid extra attention, since it can affect the performance of underwater coupler

$$C_{\mathrm{iw}} = \frac{\varepsilon_0 \varepsilon_{\mathrm{r}} S}{d}, R_{\mathrm{iw}} = \frac{\tan\delta}{\omega C_{\mathrm{iw}}} \tag{2}$$

where S is the opposite area between metal plate and seawater, ε_0 is the vacuum permittivity, ε_{r} is the relative permittivity of insulation, and d is the thickness of the insulation layer.

III. Analysis of Seawater Capacitive Coupler With Conduction Path

A. Modeling of Undersea Four-Plates Power Transfer System

In practical application, the four-plates structure is generally used to form a capacitive coupler, including the transmitting plates P_1, P_2 and receiving plates P_3, P_4. According to analysis in Section II, any plates will form a coupling capacitance with seawater, connected by seawater. Therefore, the circuit model is given in Fig. 7. There are four coupling capacitances C_{iw} (i = 12,34) and corresponding parasitic resistances R_{iw}. Since the capacitive coupling exists between each metallic plate and relevant seawater on the surface of the insulation, it results in six seawater resistances $R_{w12}, R_{w13}, R_{w14}, R_{w23}, R_{w24}$, and R_{w34} to connect them. Compared to traditional six-capacitances model in air, both special coupling mode and additional six seawater resistances need additional research. Then, according to two-port theory, the six-resistances model is simplified to a Π-model by (3) and shown in Fig. 8, imitating the calculation method of six-capacitances.

Different from the general capacitor model in air condition, the Π-resistances connecting the coupling capacitances will determine the system power transfer performance. Assuming

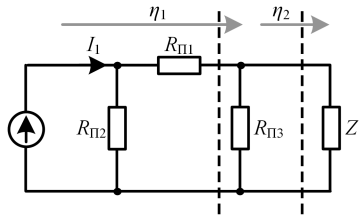

Fig. 9. Π-resistances circuit with high frequency excitation current source.

a high frequency excitation current I_1 is applied in the circuit shown in Fig. 9. Then, the equivalent internal resistance is derived and the maximum transmission power can be obtained in (5) when the impedance relationship satisfies with (4)

$$\begin{cases} R_{\Pi1} = \frac{R_{\mathrm{q}}}{R_{\mathrm{w14}}R_{\mathrm{w23}} - R_{\mathrm{w13}}R_{\mathrm{w24}}} \\ R_{\Pi2} = \frac{R_{\mathrm{w12}}R_{\mathrm{q}}}{R_{\mathrm{q}} + R_{\mathrm{w12}}(R_{\mathrm{w14}}R_{\mathrm{w24}} + 2R_{\mathrm{w13}}R_{\mathrm{w24}} + R_{\mathrm{w13}}R_{\mathrm{w23}})} \\ R_{\Pi3} = \frac{R_{\mathrm{w34}}R_{\mathrm{q}}}{R_{\mathrm{q}} + R_{\mathrm{w34}}(R_{\mathrm{w14}}R_{\mathrm{w24}} + 2R_{\mathrm{w13}}R_{\mathrm{w24}} + R_{\mathrm{w13}}R_{\mathrm{w23}})} \\ R_{\mathrm{q}} = R_{\mathrm{w14}}R_{\mathrm{w23}}R_{\mathrm{w24}} + R_{\mathrm{w13}}R_{\mathrm{w23}}R_{\mathrm{w24}} \\ \qquad + R_{\mathrm{w13}}R_{\mathrm{w14}}R_{\mathrm{w23}} + R_{\mathrm{w13}}R_{\mathrm{w14}}R_{\mathrm{w24}} \end{cases} \tag{3}$$

$$\mathrm{Re(Z)} = \frac{R_{\Pi3}(R_{\Pi1} + R_{\Pi2})}{R_{\Pi1} + R_{\Pi2} + R_{\Pi3}} \tag{4}$$

$$P_{\max} = \frac{I_1^2 R_{\Pi3}(R_{\Pi1} + R_{\Pi2})}{4(R_{\Pi1} + R_{\Pi2} + R_{\Pi3})}. \tag{5}$$

As for system efficiency, to calculate it more easily, the circuit is divided into two parts with certain efficiency, which are shown in the following equation:

$$\eta_1 = \frac{1}{\frac{R_{\Pi1}+R_{\Pi2}}{\mathrm{Re}\left(\frac{R_{\Pi3}Z}{R_{\Pi3}+Z}\right)}+1}, \eta_2 = \frac{1}{\frac{1}{R_{\Pi3}\times\mathrm{Re}\left(\frac{1}{Z}\right)}+1} \tag{6}$$

where η_1 and η_2 represent the efficiency of each part shown in Fig. 9. Moreover, based on that the parallel impedance is less than any branch impedance, the system efficiency can be expressed as follows:

$$\eta = \eta_1\eta_2 < \eta_{1\max}\eta_2 = \frac{1}{\frac{R_{\Pi1}}{R_{\Pi3}} + \frac{R_{\Pi2}}{R_{\Pi3}} + 1} \times \eta_2. \tag{7}$$

According to (5) and (7), the ability of power transfer is decided by Π-resistances $R_{\Pi1}$, $R_{\Pi2}$, and $R_{\Pi3}$, which is equivalent to seawater resistances. Considering the metallic plates are fully merged into seawater, the seawater resistance cannot be simply calculated by law of resistance. Hence, the COMSOL is used to simulate its value, depicted in Fig. 10. The distance of the same side plates is defined as d_i. It needs to be pointed out that the series-parallel resistances and occupied space of other components will inevitably affect the final result. So, a measured circuit with 300 kHz excitation voltage source U_i and four compensated inductors L_1–L_4 resonating with coupling capacitances C_{1w}–C_{4w} to eliminate their impedance is used to obtain equivalent Π-resistances. The parasitic resistance is set 0 when the dielectric dissipation factor of insulation layer is ignored. At this case, the equivalent Π-resistances $R_{\Pi1}$ and $R_{\Pi3}$ can be derived as (8). The branch current I_1 and I_4 is directly

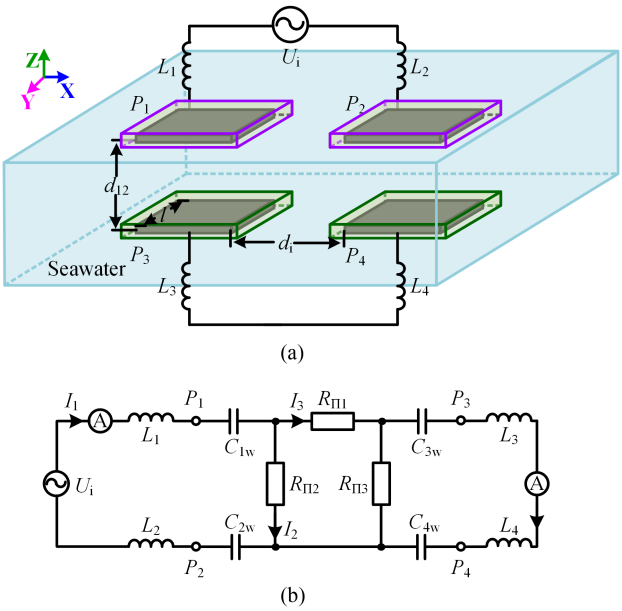

Fig. 10. (a) Three-dimensional-view of simulated model. (b) Measurement circuit of the Π-resistances with four compensated inductors and receiving short-circuited.

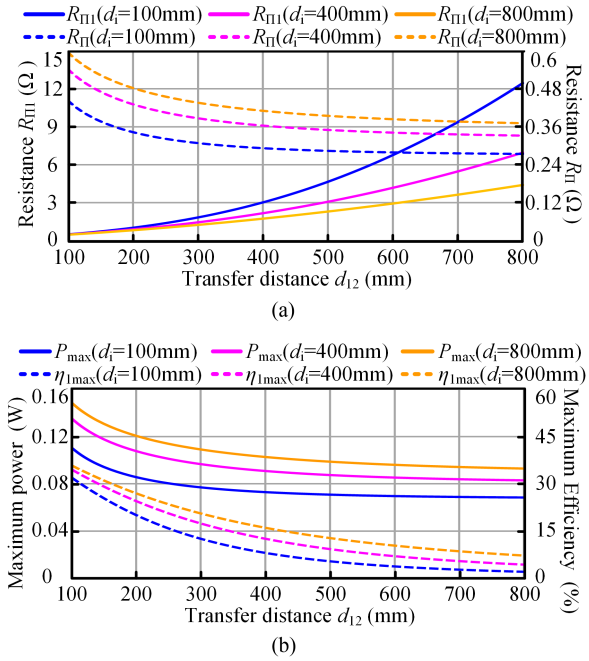

Fig. 11. Model characteristics with various transfer distance under certain ipsilateral distance. (a) Equivalent resistance. (b) Ability of power transmission.

measured and the $R_{\Pi 3}$ is equal to $R_{\Pi 2}$ due to the symmetrical coupler. Hence, at 100 mm transfer distance when plate length is set 300 mm, the equivalent resistances $R_{\Pi 1}$, $R_{\Pi 2}$, and $R_{\Pi 3}$ are separately 0.5, 0.44, and 0.44 Ω

$$R_{\Pi 1}=\frac{U_i}{I_4}, R_{\Pi 2}=\frac{U_i}{I_1-I_4}. \tag{8}$$

At this time, it can be seen that equivalent resistances are all small to milliohm, where the maximum transmission power is 0.11 W and efficiency is lower than 32% when excitation current set 1 A. It obviously hinders the power transfer. For recording the change of equivalent Π-model resistances and corresponding power transmission in detail, the stimulation results are shown in Fig. 11 when transfer distance d_{12} varies from 100 to 800 mm with ipsilateral distance set 100, 400, and 800 mm in I_1 1 A. Considering the symmetrical design, the resistance $R_{\Pi} = R_{\Pi 2} = R_{\Pi 3}$.

It shows that the resistance $R_{\Pi 1}$ quickly increases from 0.5 to 12 Ω in case of transfer distance increasing at the ipsilateral distance d_i 100 mm. As for R_{Π}, its value gradually decreases to 0.3 Ω, limited in seawater resistance R_{w12} or R_{w34} on account for parallel circuit relation. Accordingly, calculated maximum power is dozens of milliwatts and partial maximum efficiency is small in Fig. 11(b), validating the difficulty of effective power transfer. Although short transfer distance d_{12} and long ipsilateral distance d_i improve the system performance rapidly, maximum power is only 2 W with lower than 49% efficiency when d_{12} 13 mm, namely two insulation layers are close to 1 mm, under d_i 800 mm. At this time, the sensitivity of system also makes the application hard.

The influence of plates area is also considered and depicted in Fig. 12. At this time, the series resistance $R_{\Pi 1}$ reduces and

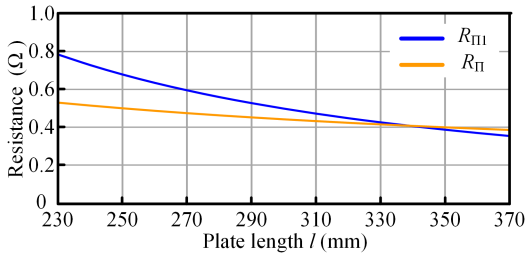

Fig. 12. Equivalent resistance variation under different plate length.

parallel resistance R_{Π} slightly changes from 0.53 to 0.39 Ω as plates length increases. Likewise, the system performance is similarly to Fig. 11(b). Combining with analysis about distance, it can be pointed that the power is difficult to transfer across seawater due to the conduction path in seawater. In other words, the parallel resistance $R_{\Pi 2}$ and $R_{\Pi 3}$ cause the subshort circuit for the back circuit as shown in Fig. 12. And because the coupler is fully integrated into the seawater, their value remains small when the size of the plate changes. So, the power mainly flows on the emission side, similar to the strong self-coupling unless the shape and distribution of the seawater is controlled to adjust the resistance.

At this time, the existed SCPT systems in [19], [20], and [21] achieving power transfer can be well explained by the model in Fig. 13. Whatever the partition damper, seawater bag or dual-cavity, they all break the parallel branch $R_{\Pi 2}$ and $R_{\Pi 3}$ at power cut-off point by physical means, leading to the power flowing in four-plates coupler.

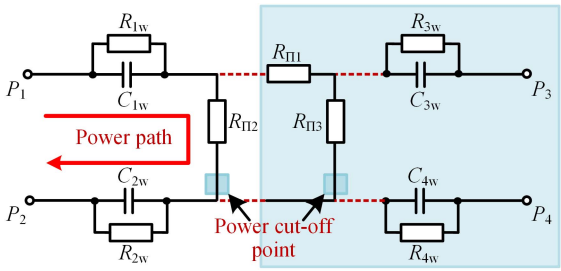

Fig. 13. Power path inside the circuit model of the undersea capacitive coupler.

B. Electric Field Distribution of the Water With Varied Conductivity

In order to validate previous analysis about distribution of displacement path ① and conduction path ② switching and the obstacles of power transfer in seawater, the electric field distribution of the four-plates at three kinds of water with different conductivity under the same excitation are shown in Fig. 14.

For better observation, the thickness of insulation is set 20 mm. It is obvious that the strength of electric of water and receiving insulation layer decreases as the water conductivity increases, indicating that conduction path ② in water gradually guides the distribution of electric field. Hence, the coupling between transmitter and receiver plates is weakened, leading to the power flowing more in emission side across insulation and water conductor, not in receiving side. In particular, faint electric field in receiving side at seawater can be attributed to conduction current according to (4). Meanwhile, considering the capacitive coupling existing between metallic objects and seawater across insulation in the marine environment, the potential power transmitted to the receiving side may flow to other circuits composed of numerous metallic objects buried in seawater. Therefore, it can be concluded that the traditional four-plates SCPT system cannot undertake the task of high-power transmission.

IV. SCPT System With Single Wire and Experiments

A. SCPT System With Y-Type Capacitor and Single Wire

According to the previous analysis, the strong self-coupling and random power transmission in seawater have become the key issues of SCPT system. To overcome them, it is necessary to divide seawater or establish an electrical identification connection. But, in the real ocean environment, it is extremely hard to divide seawater into two parts due to high pressure. Meanwhile, there are also some researches [23], [24], [25] in air using virtual connection to connect the transmitter and receiver by the stray capacitance of two large metallic blocks or long lines, rather than a real single wire. However, in the actual ocean, the seawater is connected with the ground. That means seawater also involved in the coupling and no new connection between transmitter and receiver is established. Hence, this article proposes a conductive SCPT system with double Y-type capacitors and a real single wire to achieve feasible, stable, and effective subsea power transfer. Considering an additional electrical connection added, the original circuit structure is changed. So, A basic double-sided L compensation is used and the circuit is shown in Fig. 15.

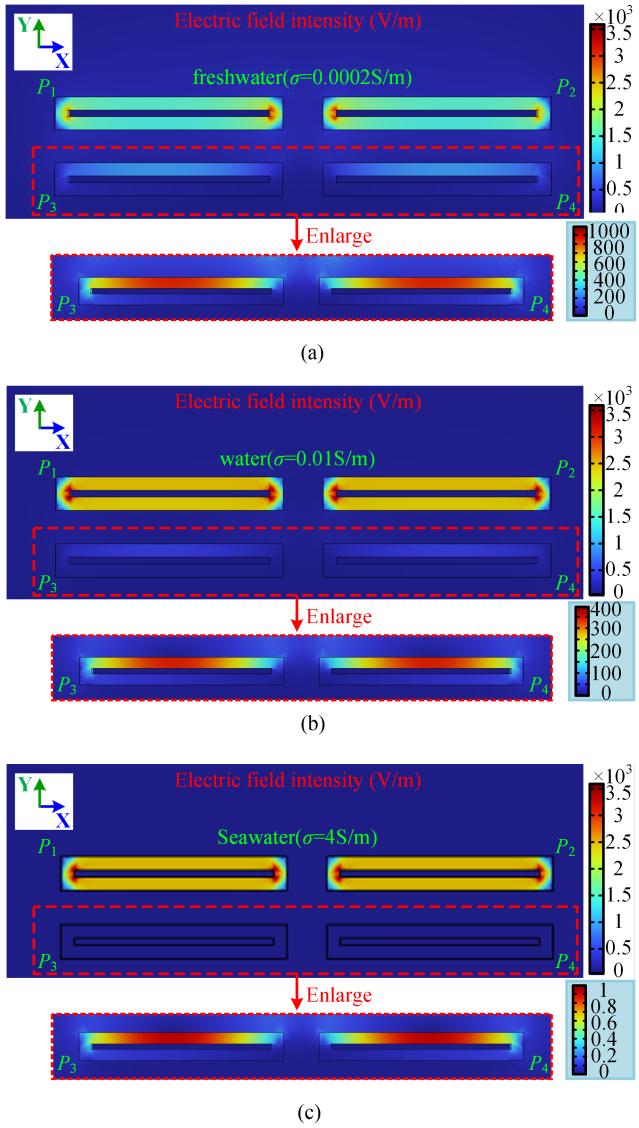

Fig. 14. Electric field distribution of underwater capacitive coupler in high frequency excitation. (a) Freshwater with σ 0.0002 S/m. (b) Water with σ 0.01 S/m. (c) Seawater with σ 4 S/m.

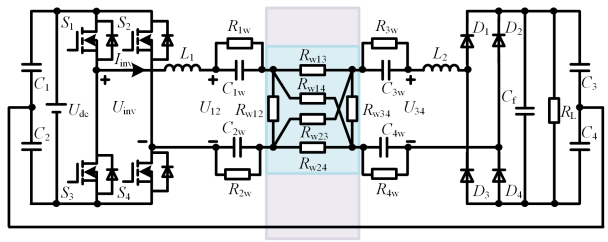

Fig. 15. Circuit topology of the capacitive coupled conductive power transfer system in seawater environment.

The double Y-type capacitors consist of four identical capacitors C_1, C_2, C_3, and C_4 with 20 nF and their midpoint is connected by a single wire to ensure the system safe when the wire exposure to seawater. At this case, a three-port network is established and an electrical potential is given in the load based on the connection, which causes the potential difference

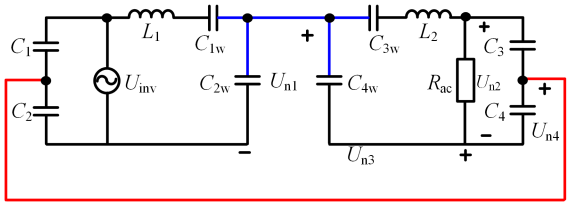

Fig. 16. Equivalent model of the proposed system.

between receiver and seawater. So, the power can flow to the expected receiving side under the reasonable circuit topology design. It needs to be noticed that the Π-model resistance is no longer applicable because the two-port structure varied. The two inductors L_1 and L_2 are utilized to compensate coupling capacitance and eliminate reactive power. By testing in circuit simulation software, an approximate equivalent circuit model is illustrated in Fig. 16, ignoring the parasitic parameters and seawater resistance due to their small value, and a resonant relationship is given in the following equation:

$$\omega^2 L_1 \frac{C_{1w} \times C_{2w}}{C_{1w}+C_{2w}} = 1, \omega^2 L_2 \frac{C_{3w} \times C_{4w}}{C_{3w}+C_{4w}} = 1. \quad (9)$$

When the negative terminal of the power supply is set as the reference point, according to KCL, the circuit equations can be listed and by substituting (9) into these, the output voltage is derived as shown in (10). It is important to note that since the single wire connects the midpoint of the double Y-type capacitors in both the source and the load, this will have an impact on both the inverter and the rectifier. In future, the working principle of conductive circuit will be further studied

$$U_R = -\frac{C_{2w}}{C_{4w}} U_{dc}. \quad (10)$$

As shown in Fig. 17, the current density in SCPT system with or without single wire is tested in COMSOL to describe the working principle. It can be seen that the current mainly flows in the transmitter without single wire, leading to weak power transmission capacity. But when the single wire is added, the current in seawater is guided to the receiver and returns by the single wire, showing strong current density in the receiving plate. This makes it possible to realize SCPT for submarine equipment with metal shell.

B. Laboratory Experiment

To verify the previous analysis, a prototype of SCPT system without or with single wire is implemented based on the above-mentioned circuit topology, as shown in Fig. 18.

In the prototype, four aluminum plates with soda lime glass covering them as insulation constitute the capacitive coupler, as structured in Fig. 1(a). Since the rectangular glass is attached to the plate, the gap between them is filled by the acidic glass cement with corrosion resistance. Similar to the area of the mentioned plate, the size of plates P_1–P_4 is set 500 × 160 × 1 mm and the thickness of insulation layer is 1 mm. Then, the coupler is merged into seawater and fixed by plastic slot. At this time, both of the distance between ipsilateral plates d_s and distance

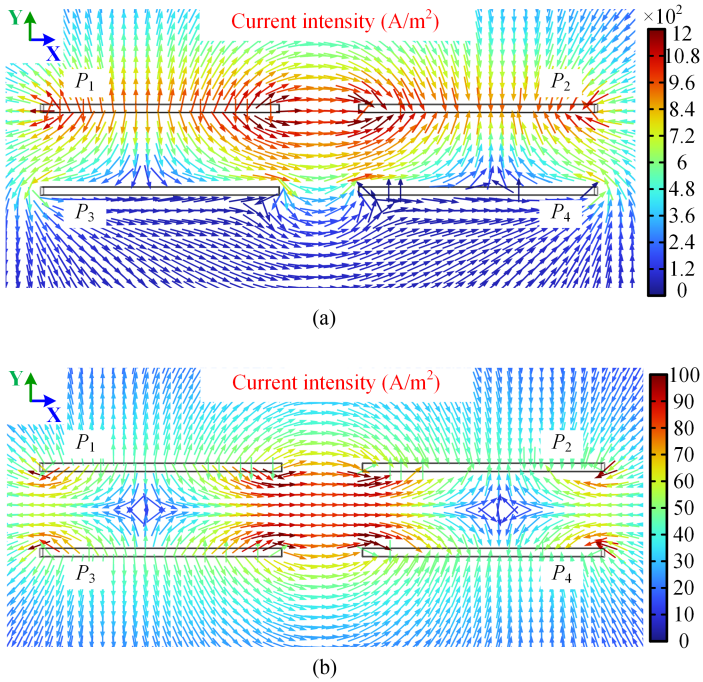

Fig. 17. Current intensity of underwater CPT system (a) without single wire and (b) with single wire.

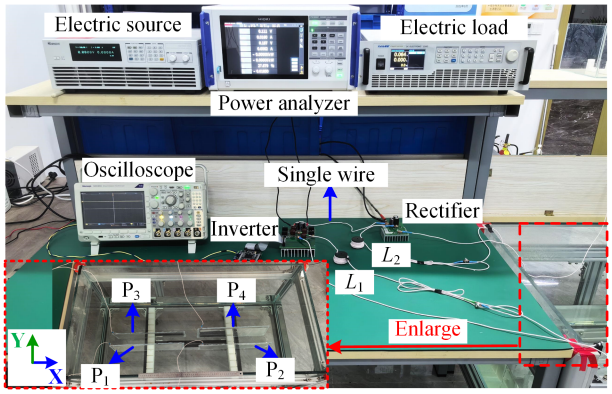

Fig. 18. Prototype of the SCPT system with single wire.

between opposite plates d_{12} can vary from 100 to 500 mm. Therefore, the relative position of plates can be easily changed to test system performance. Meanwhile, the wire is connected to the aluminum plate by screws and the connection point is exposed to air possessing good insulation.

For capacitive coupler in seawater environment, the system parameters are measured by impedance analyzer. It should be noted that the coupling capacitances across insulation and the parasitic resistances can be directly obtained by setting metal terminal on the insulation surface and the seawater resistances are hard to measure accurately due to additional resistance and small value. Hence, only approximate seawater resistance can be given. Although the measurement is slightly different from the theoretical analysis considering production and measuring precision, the output power and efficiency is still small, agreed

TABLE II
CIRCUIT PARAMETER OF CONDUCTIVE SCPT SYSTEM

Parameter	Value	Parameter	Value	Parameter	Value
U_{dc}	120 V	f	300 kHz	R_L	10–80 Ω
C_{1W}	10 nF	C_{2W}	10.31 nF	C_{3W}	10.29 nF
R_{1w}	2.52 kΩ	R_{2w}	2.379 kΩ	R_{3w}	2.554 kΩ
C_{4W}	10.3 nF	L_1	58.3 μH	L_2	54.68 μH
R_{4w}	2.35 kΩ	d_s	100 mm	d_{12}	100 mm
$R_{Π1}$	0.81 Ω	$R_{Π2}$	0.53 Ω	$R_{Π3}$	0.76 Ω

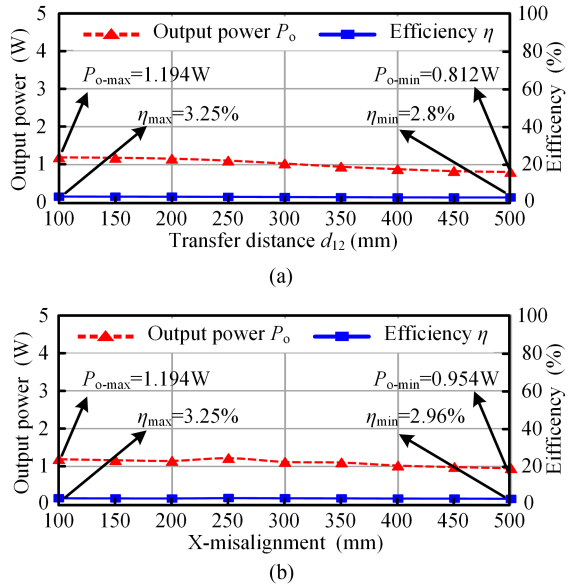

Fig. 19. System performance of power transfer and efficiency with no single wire. (a) Varied transfer distance. (b) X-misalignment.

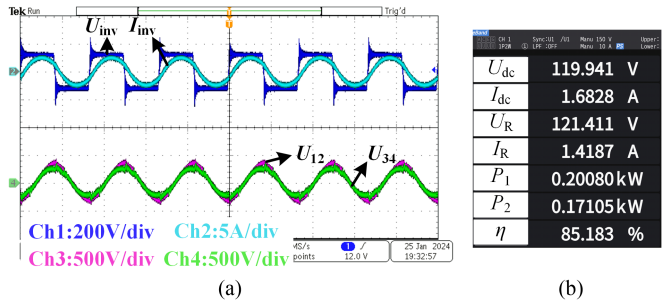

Fig. 20. (a) Experimental waveforms of input voltage and current and plates voltage. (b) Tested power and efficiency of conductive SCPT system.

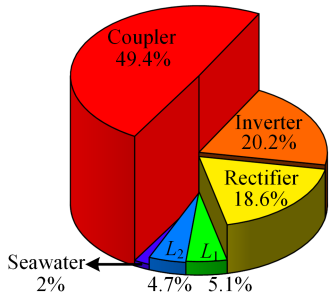

Fig. 21. Power loss distribution of the experimental prototype.

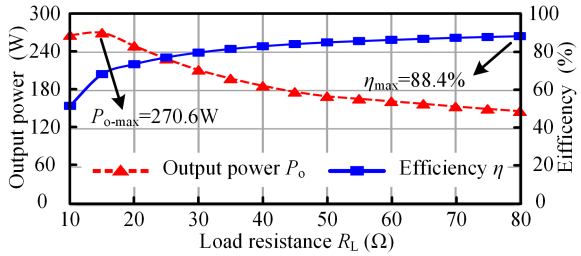

Fig. 22. System output power and efficiency under varied load resistance.

well with previous analysis in Section III-A. According to (9), the resonant inductors can be calculated and the primary inductor is set larger to satisfy zero voltage switch (ZVS) for reducing the loss of inverter. At this case, the system parameter is listed in Table II. The working frequency is chosen 300 kHz since the value of the coupling capacitance is high and input voltage is set 120 V.

First, the SCPT system without single wire is tested under different transfer distance and lateral misalignment. It is noted that the input voltage is set 20 V to avoid the risk of large power loss and potential electrical breakdown since the power mainly flows in the transmitting side. The results are shown in Fig. 19 and it can be pointed that only few powers with low efficiency can be transmitted to the load and nearly unaffected by transfer distance and misalignment, validating weak capacity of power transmission.

And then, when the coupler in water tank is aligned with single wire, the experimental waveform and the system transmission performance are obtained, as shown in Fig. 20. It can be seen that the input current I_{inv} slightly lags input voltage U_{inv}, achieving ZVS. And the plates voltage U_{12} and U_{34} are almost consistent, indicating that the power is successfully transmitted from the transmitting side to receiving side in seawater environment. The voltage between plates and seawater is also tested with the maximum peak value of 0.2 kV. Since the dielectric strength of soda lime glass is nearly 10 kV/mm, 1 mm thickness insulation can ensure the system safety operation. Moreover, the output power reaches 171 W with the efficiency of 85%, validating the effectiveness of the conductive SCPT system power transmission.

The power loss distribution of the conductive SCPT system is obtained in Fig. 21 based on the measurement and datasheet. It can be pointed that the power loss is mainly attributed by coupler parasitic resistance with 14.7 W. Besides, the power loss in seawater is small to 2%, leading to the possibility of long-distance power transfer under the single wire since only seawater resistances are affected by transmission distance in SCPT system. Of course, in practical application, the long single wire merged into seawater environment will have inevitable effect on the system performance.

The measured system property with variable load resistance is shown in Fig. 22. It can be seen that the output power varies from 270 to 148 W because of constant voltage output

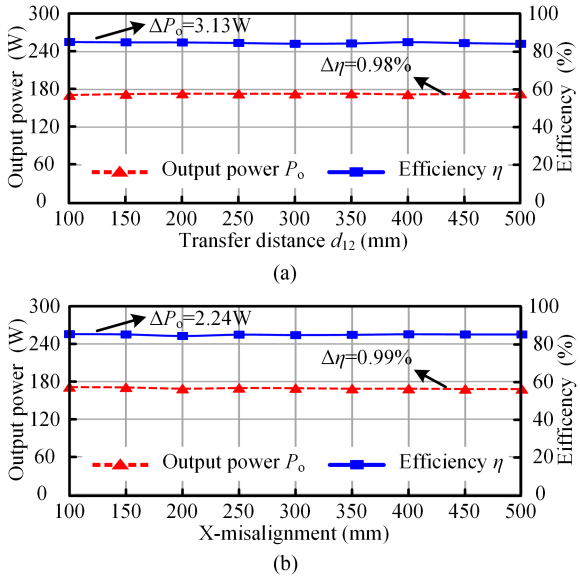

Fig. 23. System performance of power transfer and efficiency. (a) Varied transfer distance. (b) X-misalignment.

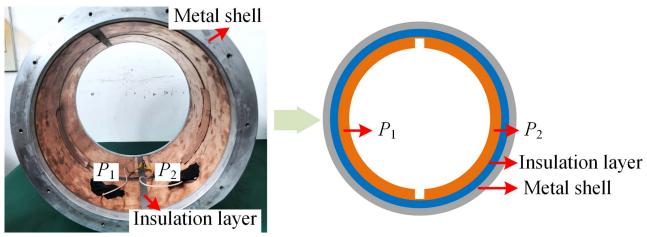

Fig. 24. Capacitive coupler with metal shell in the actual ocean.

in (8) and the system efficiency increases from 52% to 88.4%, showing prosperous ability of energy transfer. The reason of low efficiency at small load resistance may be large parasitic resistance and simple series-series compensated topology.

As for the coupler misalignment occasion, the experimental results are shown in Fig. 23 when the transfer distance and lateral misalignment separately occurs. At this case, 50 Ω load resistance is chosen. It can be pointed that whatever output power or efficiency keeps stable when relative location varies. Hence, the SCPT system with single wire has large potential for unmanned equipment in marine environment.

C. Actual Ocean Experiment

Considering that the actual ocean is more complex than the water tank in the laboratory, this article makes a new undersea capacitive coupler with metal shell and constructs an actual ocean experiment for further verifying the analysis. As shown in Fig. 24, an insulation layer with silicone pad is first attached to the metal shell to isolate the connection of copper foil and metal shell. And then the copper foils are used as plate to form the coupler and the coupling capacitance between two copper foils can be ignored considering the strong coupling between

TABLE III
CIRCUIT PARAMETER OF UNDERSEA COUPLER

Parameter	Value	Parameter	Value	Parameter	Value
C_{1w}	10.18 nF	C_{2w}	8.93 nF	C_{3w}	9.0 nF
R_{1w}	1.51 kΩ	R_{2w}	1.76 kΩ	R_{3w}	1.65 kΩ
C_{4w}	10 nF	$R_{\Pi 1}$	0.92 Ω	$R_{\Pi 2}$	1 Ω
R_{4w}	1.56 kΩ	$R_{\Pi 3}$	0.91 Ω		

Fig. 25. Prototype of the SCPT system with single wire in the actual ocean.

copper foils and metal shell based on the small thickness of the insulation layer. Finally, the metal cabin is sealed and the connection is drawn through the watertight joint. Then putting the metal cabin in the ocean and the measurement results are listed in Table III. Correspondingly, there only the power of 0.15 W with no more than 32.15% efficiency can be transmitted to the receiver when the input current 1 A. Obviously, a little of difference exists because the deviated plate area and manual fabrication error. But the results can still prove the weak power transmission for SCPT system without additional method.

Then the inverter, compensated circuit and rectifier are all encapsulated in the metal shell and conducting an actual ocean experiment with 10 m transfer distance, shown in Fig. 25. The transmitter and receiver are fully immersed into the sea and all the connection lines have been waterproofed. To provide clear illustration, a yellow LED strip is attached to the single wire, and using different lights to distinguish the transmitter and receiver. A 50 Ω resistor is used as the load and the multimeter can measure the output voltage for conveniently testing. So, the output performance like power and efficiency can be calculated correspondingly. When the input voltage set 100 V, the output power reaches 135.4 W with the efficiency of 74.4%. It is slightly different with the laboratory experiment and the reason can may be attributed to the ground or the effect of parasitic parameter of components. But the phenomenon can prove the system proposed in this article can be applied in the actual ocean and promote the development of SCPT system applications.

D. Comparative Analysis

To highlight the advantages and disadvantages of the proposed SCPT system with single wire, various state of-the-art power transfer technologies are compared below.

Advantages: 1) Reducing the complexity of aligning, connecting, and sealing for underwater connectors as it tolerates a certain amount of seawater ingress without the risk of short-circuiting. 2) Avoiding the risk of electrical breakdown and rope damage between the parallel transmission lines.

Disadvantages: 1) A relatively high loss due to partial wireless power transmission. 2) The installation difficulty, operational challenges, and wear of the interface are relatively decreased but still exist.

Currently, the efficient power supply for the marine equipment is mainly achieved through wireless charging or wet mate technology. However, for the wireless charging technology, when the shell is constructed by conductive material, the previous research for SCPT technology in [18], [19], [20], and [21], and IPT technology is hard to achieve due to large leakage current and eddy loss. As for the wet mate technology, it is required that connection and disconnection can be performed underwater, typically by underwater robots [26], [27]. This technology can well be applied to marine equipment but the issues such as high installation difficulty, operational challenges and easy wear of the interfaces are inevitable partially due to two or more conductors are jointed and other seawater environmental impacts. So, the proposed seawater CPT technology with single wire aims to advance the technology from electrical perspective and reduce the difficulty of implementation. It can promote the development of SCPT system in undersea applications.

V. Conclusion

This article proposed a circuit model of undersea four-plates coupler, which is completely immersed in seawater, with four independent coupling capacitances and six resistances. The circuit model was analyzed and simulated by COMSOL and the difficulty of power transmission in the SCPT system was verified. A conductive SCPT system with Y-type capacitor and single wire was given to achieve power transfer. And then, a laboratory prototype was first built to validate analysis. It proved the weak power transmission without single wire and achieved stable 171 W power transmission and 85% efficiency under random misalignment in X- or Y-directions with single wire. Also, an actual ocean experiment is constructed and the experimental results show the proposal can be well promoted the practical applications of SCPT system.

References

[1] H. T. Nguyen et al., "Review map of comparative designs for wireless high-power transfer systems in EV applications: Maximum efficiency, ZPA, and CC/CV modes at fixed resonance frequency independent from coupling coefficient," *IEEE Trans. Power Electron.*, vol. 37, no. 4, pp. 4857–4876, Apr. 2022.

[2] S. Wu, C. Cai, W. Chai, J. Li, Q. Cui, and S. Yang, "Uniform power IPT system with quadruple-coil transmitter and crossed dipole receiver for autonomous underwater vehicles," *IEEE Trans. Ind. Appl.*, vol. 58, no. 1, pp. 1289–1297, Jan./Feb. 2022.

[3] Z. Yan et al., "Frequency optimization of a loosely coupled underwater wireless power transfer system considering eddy current loss," *IEEE Trans. Ind. Electron.*, vol. 66, no. 5, pp. 3468–3476, May 2019.

[4] S. Wu, C. Cai, A. Wang, Z. Qin, and S. Yang, "Design and implementation of a uniform power and stable efficiency wireless charging system for autonomous underwater vehicles," *IEEE Trans. Ind. Electron.*, vol. 70, no. 6, pp. 5674–5684, Jun. 2023.

[5] Y.-G. Su, S.-Y. Xie, A. P. Hu, C.-S. Tang, W. Zhou, and L. Huang, "Capacitive power transfer system with a mixed-resonant topology for constant-Current multiple-pickup applications," *IEEE Trans. Power Electron.*, vol. 32, no. 11, pp. 8778–8786, Nov. 2017.

[6] Y. Naka, K. Yamamoto, T. Nakata, M. Tamura, and M. Masuda, "Verification efficiency of electric coupling wireless power transfer in water," in *Proc. IEEE MTT-S Int. Conf. Microw. Intell. Mobility*, 2017, pp. 83–86.

[7] M. Urano, K. Ata, and A. Takahashi, "Study on underwater wireless power transfer via electric coupling with a submerged electrode," in *Proc. IEEE Int. Meeting Future Electron Devices*, 2017, pp. 36–37.

[8] M. Tamura, Y. Naka, and K. Murai, "Design of capacitive coupler for wireless power transfer under fresh water focusing on kQ product," in *Proc. IEEE/MTT-S Int. Microw. Symp.*, 2018, pp. 1257–1260.

[9] M. Tamura, Y. Naka, K. Murai, and T. Nakata, "Design of a capacitive wireless power transfer system for operation in fresh water," *IEEE Trans. Microw. Theory Techn.*, vol. 66, no. 12, pp. 5873–5884, Dec. 2018.

[10] H. Zhang and F. Lu, "Feasibility study of the high-power underwater capacitive wireless power transfer for the electric ship charging application," in *Proc. IEEE Electric Ship Technol. Symp.*, 2019, pp. 231–235.

[11] H. Zhang and F. Lu, "Insulated coupler structure design for the long-distance freshwater capacitive power transfer," *IEEE Trans. Ind. Inform.*, vol. 16, no. 8, pp. 5191–5201, Aug. 2020.

[12] H. Li, G. Li, X. Jin, J. Li, and G. Xu, "A LC-CLL compensated capacitive wireless power transfer system in fresh water," in *Proc. 5th Int. Conf. Power Energy Appl.*, 2022, pp. 130–137.

[13] E. Rong, P. Sun, K. Qiao, X. Zhang, G. Yang, and X. Wu, "Six-plate and hybrid-dielectric capacitive coupler for underwater wireless power transfer," *IEEE Trans. Power Electron.*, vol. 39, no. 2, pp. 2867–2881, Feb. 2024.

[14] R. Sedehi et al., "A wireless power method for deeply implanted biomedical devices via capacitively coupled conductive power transfer," *IEEE Trans. Power Electron.*, vol. 36, no. 2, pp. 1870–1882, Feb. 2021.

[15] M. Tamura, K. Murai, and Y. Naka, "Capacitive coupler utilizing electric double layer for wireless power transfer under seawater," in *Proc. IEEE MTT-S Int. Microw. Symp.*, 2019, pp. 1415–1418.

[16] K. Murai and M. Tamura, "Improvements of transfer efficiency in capacitive wireless power transfer under seawater," in *Proc. IEEE Asia-Pacific Microw. Conf.*, 2019, pp. 714–716.

[17] M. Tamura, K. Murai, and D. Fujii, "Lightweight and high-efficiency coupler suitable for underwater WPT system," in *Proc. IEEE Asia-Pacific Microw. Conf.*, 2019, pp. 7–9.

[18] M. Tamura, K. Murai, and M. Matsumoto, "Conductive coupler for wireless power transfer under seawater," in *Proc. IEEE/MTT-S Int. Microw. Symp.*, 2020, pp. 1176–1179.

[19] M. Tamura, K. Murai, and M. Matsumoto, "Design of conductive coupler for underwater wireless power and data transfer," *IEEE Trans. Microw. Theory Techn.*, vol. 69, no. 1, pp. 1161–1175, Jan. 2021.

[20] L. Yang, M. Ju, and B. Zhang, "Bidirectional undersea capacitive wireless power transfer system," *IEEE Access*, vol. 7, pp. 121046–121054, 2019.

[21] H. Mahdi, B. Hoff, P. G. Ellingsen, and T. Østrem, "Conformal transformation analysis of capacitive wireless charging," *IEEE Access*, vol. 10, pp. 105621–105630, 2022.

[22] L. Holysz, A. Szczes, and E. Chibowski, "Effects of a static magnetic field on water and electrolyte solutions," *J. Colloid Interface Sci.*, vol. 316, no. 2, pp. 996–1002, 2007.

[23] X. Gao et al., "Capacitive power transfer through virtual self-capacitance route," *IET Power Electron.*, vol. 11, no. 6, pp. 1110–1118, 2018.

[24] L. J. Zou, Q. Zhu, C. W. V. Neste, and A. P. Hu, "Modeling single-wire capacitive power transfer system with strong coupling to ground," *IEEE J. Emerg. Sel. Topics Power Electron.*, vol. 9, no. 2, pp. 2295–2302, Apr. 2021.

[25] Z. Liu, H. Hu, Y.-G. Su, Y. Sun, F. Chen, and P. Deng, "A double-receiver compact SCC-WPT system with CV/CC output for mobile devices charging/supply," *IEEE Trans. Power Electron.*, vol. 38, no. 7, pp. 9230–9245, Jul. 2023.

[26] W. Song and W. Cui, "An overview of underwater connectors," *J. Mar. Sci. Eng.*, vol. 9, no. 8, 2021, Art. no. 813.

[27] F. Rémouit, P. Ruiz-Minguela, and J. Engström, "Review of electrical connectors for underwater applications," *IEEE J. Ocean. Eng.*, vol. 43, no. 4, pp. 1037–1047, Oct. 2018.

Xichen Liu (Student Member, IEEE) was born in Shandong Province, China, in 1998. He received the B.S. and M.S. degrees, in 2020 and 2023, respectively, in electrical engineering from Harbin Institute of Technology, Weihai, China, where he is currently working toward the Ph.D. degree in electrical engineering.

His current research interests include power electronics and wireless power transfer system for autonomous underwater vehicles and unmanned aerial vehicles.

Chunwei Cai (Member, IEEE) was born in Shandong Province, China, in 1977. He received the B.S. and M.S. degrees in control theory and control engineering from Shan Dong University, Jinan, China, in 2001 and 2004, respectively, and the Ph.D. degree in electrical engineering from Harbin Institute of Technology (HIT), Harbin, China, in 2013.

He has been a Lecturer with HIT, Weihai, China, since 2006. Since 2014, he has been working as a Professor with HIT, Weihai, China. His current research interests include wireless power transfer systems, power converters, and inverters.

Shuai Wu (Member, IEEE) was born in Shanxi Province, China, in 1995. He received the B.S. degree in electrical engineering and automation from Shanxi Agricultural University, Jinzhong, China, in 2017, and the M.S. and Ph.D. degrees in electrical engineering from the Harbin Institute of Technology (HIT), Harbin, China, in 2019 and 2023, respectively.

Since 2023, he has been an Associate Professor with the School of New Energy, HIT, Weihai, China. His current research interests include wireless power transfer for unmanned vehicles and implanted biomedical devices.

Chenghao Li (Graduate Student Member, IEEE) was born in Liaoning Province, China, in 2000. He received the B.S. degree in electrical engineering, in 2023, from Harbin Institute of Technology, Harbin, China, where he is currently working toward the Ph.D. degree in electrical engineering.

His current research interests include long-distance seawater capacitive power transfer, mechanism of electromagnetic field, and simultaneous wireless power and data transfer.

Qinyuan Cui received the B.S. and M.S. degrees in electrical engineering and automation from Harbin Institute of Technology, Weihai, China, in 2020 and 2022, respectively.

He currently works with State Grid Zhejiang Electric Power Company Ltd., Hangzhou Power Supply Company, Hangzhou, China. His current research interest focuses on wireless power transfer.

Xiuyun Ren (Member, IEEE) received the B.A. degree in physics and the M.S. degree in optics from Shandong Normal University, Jinan, China, in 2002 and 2005, respectively, and the Ph.D. degree in physical electronics from the Harbin Institute of Technology, Harbin, China, in 2016.

Since 2014, she has been an Associate Professor with the School of Information Science and Engineering, Harbin Institute of Technology, Weihai, China. Her research interests include Lidar ocean exploration, wireless communication technology, and optoelectronic technology and their applications.